# It's not just a phase: crystallization and X-ray structure determination of bacteriorhodopsin in lipidic cubic phases

Eric Gouaux

Utilization of lipidic cubic phases in the crystallization of bacteriorhodopsin (bR) has yielded long sought after crystals that diffract X-rays to 2 Å resolution. The resulting structure provides new information on the protein conformation and the mechanism of proton translocation. Crystallization of bR via lipidic cubic phases may be a harbinger of new membrane protein crystallization strategies.

Address: Department of Biochemistry and Molecular Biophysics, Columbia University, 650 West 168th Street, New York, NY 10032, USA.

E-mail: jeg52@columbia.edu

Structure 15 January 1998, 6:5–10
http://biomednet.com/elecref/0969212600600005



*We dance round in a ring and suppose,*
*But the Secret sits in the middle and knows* [1].

## Overview

Well ordered, three-dimensional (3D) crystals of bacteriorhodopsin (bR) from *Halobacterium salinarium* have eluded protein crystallographers since the late 1970s. Recently, small crystals of bR were grown using a novel crystallization strategy based on lipidic cubic phases. The bR crystals are composed of membrane-like two-dimensional (2D) sheets stacked perpendicular to the *c* axis of the $P6_3$ unit cell. Extensive lipid-mediated contacts between the transmembrane portions of the protein as well as polar contacts between the solvent-exposed loops help to stabilize the crystals. By utilizing an intense microfocus synchrotron X-ray beam, diffraction data were observed to 2.0 Å resolution and a data set was collected to 2.4 Å resolution. The resulting structure better defines key residues and solvent molecules implicated in proton transfer. Application of lipidic cubic phases to membrane protein crystallization, although presently limited in success to bR, represents a conceptual breakthrough and may prove to be an invaluable tool.

## bR as a paradigm

Discovered by Oesterhelt and Stoeckenius in 1971 as the sole protein component of the purple membrane from *H. salinarium* [2], and initially characterized using electron microscopy by Blaurock and Stoeckenius [3], bR was christened after its namesake, rhodopsin, due to the presence of retinal as the chromophore. As one of the first polytopic membrane proteins studied at the molecular level, bR has ridden the crest of one wave of experiments after another, washing a rich tide of information and knowledge ashore. Garnered from these experiments are insights into the structure, function, folding and stability of bR and, by analogy, into other integral membrane proteins.

Shortly after the characterization of purple membrane, Henderson and Unwin began the task of structure determination by electron diffraction methods [4], which have recently culminated in molecular structures [5,6]. In 1977 Gobind Khorana's laboratory reported that bR remained intact after solubilization in detergent and complete delipidation [7]. Subsequently, Khorana and coworkers showed that the purple protein–retinal complex, isolated from detergent-solubilized purple membrane, could be completely denatured and refolded [8]. Khorana and Ovchinnikov individually determined the polypeptide sequence, thus defining another landmark [9,10]. Khorana continued with the complete synthesis of the bR gene and, along with Oesterhelt, Lanyi and others, carried out cycles of site-directed mutagenesis and biophysical characterization [11–13]. Yet in spite of untold efforts, well ordered, 3D crystals of bR were not grown until recently [14], even though bR had yielded one of the first membrane protein crystals [15], and later had been coaxed to produce other modestly ordered forms (see for example [16]).

## Crystallization

From one of the first reports of the crystallization of a membrane protein [17] up to about one year ago, Rosenbusch and colleagues pursued the crystallization and structural study of membrane proteins using the conventional strategy of crystallization of protein–detergent micelle complexes [18]. One year ago, however, Landau and Rosenbusch reported the crystallization of bR via a novel method that does not involve the crystallization of protein–detergent micelle complexes [14,19]. Instead, the method that Landau and Rosenbusch employed exploited the continuous lipid bilayer present in one type of lipidic cubic phase.

Lipidic cubic phases are lipid and water mixtures that display cubic symmetry [20,21]. Currently, seven distinct cubic phases have been characterized [22]. Two major subtypes of lipidic cubic phases are 'micellar' and 'bicontinuous'. The micellar class consists of discontinuous hydrophobic regions (micelles) separated by polar interstices while the bicontinuous class contains a complex interconnecting bilayer (Figure 1). The $Q^{224}$ bicontinuous lipidic cubic phase (space group $Pn3m$), which is formed by 1-monooleoyl-*rac*-glycerol, 1-monopalmitoleoyl-*rac*-glycerol, as well as by other lipids, is the phase that promoted the 3D crystallization of bR. Interestingly, the

**Figure 1**

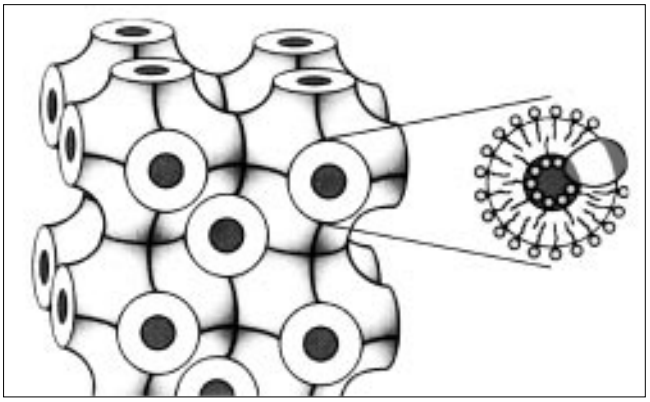

Schematic model of a bicontinuous lipidic cubic phase belonging to the space group *Im3m*. This lipidic cubic phase is deemed bicontinuous because the water and lipid elements are continuous with respect to both components. Here, the elements are water, lipid and a membrane protein. This lipidic phase is composed of a continuous bilayer surface interpenetrated by a connecting series of aqueous channels, shown in dark gray. An enlarged section on the right-hand side of the figure shows how a membrane protein (oval) might interact with the curved bilayer and the central aqueous channel. In the lipidic cubic phase employed in the growth of bR crystals, both membrane-associated and water-solvated components can diffuse freely through the membrane and aqueous channels, respectively, at room temperature. (The figure and legend were adapted from [14] with permission.)

**Figure 2**

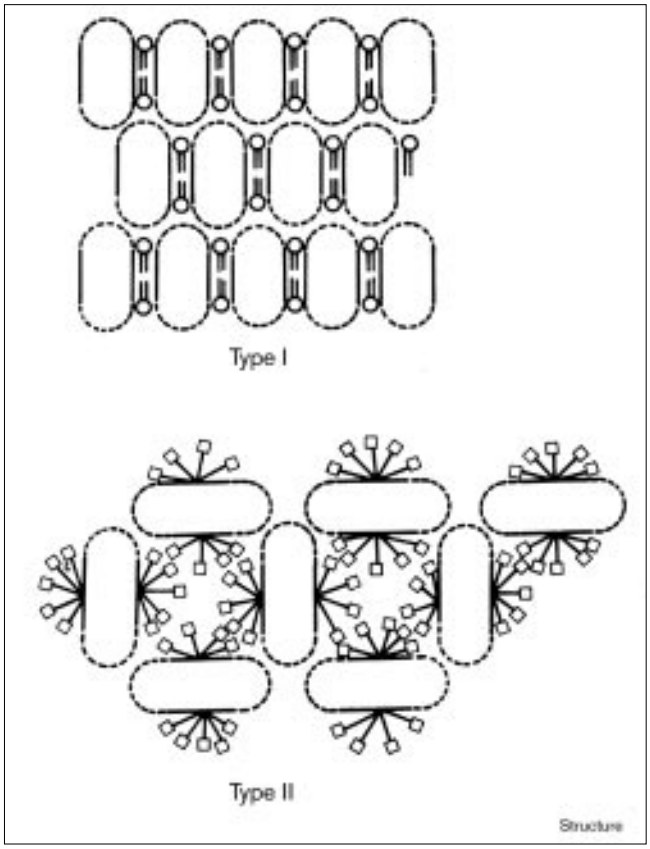


Schematic representation of two types of membrane protein crystals [24]. Type I are two-dimensional sheets of membrane-like crystals stacked in the third dimension. In type I crystals, lattice interactions are both of a hydrophilic and hydrophobic nature. This type of packing is found in the crystals of bR grown from lipidic cubic phases. Type II crystals are formed by protein–detergent complexes and lattice contacts consist primarily of interactions between the polar portions of the membrane protein. Detergent and aqueous solvent fill the interstices. In general, type II crystals have a high solvent content and $V_M$ values [34] that are substantially larger than those observed for water-soluble proteins.

$Q^{224}$ phase has been identified *in vivo* and it may provide an efficient and compact arrangement of lipids and membrane in a 3D space [23].

Formation of a 3D lattice by means of stacking membrane-like sheets of 2D crystals (so-called type I crystals; see Figure 2 and [24]) has been a goal in the field of membrane protein crystallography for some time (see for example [25]). Although previous attempts to grow type I crystals have generally been unsuccessful, lattices that approximate stacks of 2D sheets have been observed [26]. Most 3D membrane protein crystals characterized to date, however, are of the type II variety [24], in which the hydrophobic, transmembrane portion of the protein is surrounded by a detergent micelle and participates in only a few, if any, protein–protein contacts. In contrast, type I crystals contain extensive contacts between both the polar and nonpolar portions of the protein.

As suggested by Landau and Rosenbusch, bicontinuous lipidic cubic phases offer a crystallization milieu that can provide sites for crystal nucleation and can support growth of the crystal seed [14]. The lipid membrane in the type $Q^{224}$ phase could allow for the propagation of the crystal latice by lateral diffusion of the protein molecules [14]. Although as yet there is no experimental evidence for the mechanism of growth of bR crystals in the lipidic cubic phase, reasonable speculations are that 2D crystals, or patches of 2D crystals form first, and then the 2D lattices grow or stack in the third dimension. The bR crystals are densely packed and contain 62% protein by volume [27]. Thus, the lipidic phase may deform, and possibly reform, to allow for the continual deposition of protein molecules into the growing and tightly-packed lattice.

The plane perpendicular to the sixfold screw axis in the 3D crystals, and the plane perpendicular to the threefold axis in the 2D crystals are almost in exact correspondence. This observation, combined with the knowledge that *H. salinarium* lipids facilitate growth of 2D crystals [28], leads one to ask if one or a few tightly bound *H. salinarium* lipids, which might have remained bound to the protein throughout

purification of the bR monomer, mediate key contacts in the 3D crystals. Perhaps protein–lipid and lipid–lipid interactions will play a particularly important role in the formation of type I crystals via the lipidic cubic phase.

Crystallization of bR in the lipidic cubic phase results in the growth of hundreds of hexagonal plates per crystallization vial; typical dimensions are 20–40 μm × 20–40 μm × 5 μm [27]. Aided by their bright purple color, the crystals were isolated, flash-cooled to 100K and characterized at the microfocus beam line ID13 at the European Synchrotron Radiation Facility [27]. Diffraction quality varied substantially from crystal to crystal and only 10% of the crystals diffracted to 2.0 Å resolution; the thickest plates had a mosaicity of several degrees while the thinner plates were more well ordered and had a mosaicity an order of magnitude smaller [27]. This variability in crystal quality, which is much greater than that seen with water-soluble proteins, is frequently observed with membrane proteins. The space group of the crystals is $P6_3$ and the unit-cell dimensions are $a = b = 61.76$ Å, $c = 104.16$ Å and $\gamma = 120°$ [27]. These values show a striking correspondence to those of the naturally occurring 2D crystals from purple membrane which have the layer group P3 and unit-cell dimensions $a = b = 62.45$ Å, $c = 100$ Å and $\gamma = 120°$ [4–6].

**Crystal structure**

Overall, the structure of bR determined from the lipidic cubic phase crystals is similar to the structure of bR determined by electron crystallography, although there are some differences in loop conformation and sidechain orientation (Figure 3). The structure was solved by molecular replacement using the coordinates of Henderson and colleagues as a search model [5]. After limited refinement of atomic positions and temperature factors, using data between 5 and 2.5 Å resolution ($F > 3\sigma$, 5893 reflections), the resulting structure yielded a conventional R value of 0.221 and a free R value of 0.327 with good stereochemistry [27].

As implied by the correspondence between the unit-cell dimensions of the 3D and 2D crystal forms, the arrangement of the monomeric species in the (*a*,*b*) plane is similar in both crystal forms. Moreover, the trimers are arranged in a manner indistinguishable from that of the trimer arrangement in purple membrane, as illustrated in Figure 4. Interactions between loops AB and CD, and contacts between helices B and D form the most extensive contacts within a trimer. In fact, Krebs and coworkers have demonstrated that intratrimer hydrophobic contacts between helices B and D are important for the formation and stability of the purple membrane lattice [29]. When

**Figure 3**

Intertrimer packing of bR showing the interactions within layers in the (*a*,*b*) plane and between layers. The (*a*,*b*) plane is perpendicular to the *c* axis and corresponds to the bilayer plane of purple membrane. There are no protein–protein contacts between trimers in the (*a*,*b*) plane; these interactions must be mediated by lipids. Between layers there are only a few protein–protein interactions and they involve loops AB and BC, as shown in inset I. Inset II is a space-filling representation of region II. The color coding for atoms is: carbon, yellow; oxygen, red; nitrogen, blue; sulfur, green. (The figure and legend were adapted from [27] with permission.)

**Figure 4**



Illustration of bR trimers in the (*a*,*b*) plane, oriented to mimic a view from the cytoplasmic surface towards the extracellular space. Emphasized in the upper right protomer are the positions of the helices and the connecting loops, the latter being shown as solid lines on the cytoplasmic side and as dashed lines on the extracellular side. In the upper left protomer the backbone of the α helices is drawn in green. The lower protomer illustrates the extensive intratrimer contacts mediated by loops AB and CD, using the same color code as in Figure 3. (The figure and legend were adapted from [27] with permission.)

comparing the X-ray structure [27] and the electron diffraction structure of Grigorieff *et al.* [5], the AB and BC loops are the most different in conformation, although the molecular basis for this divergence is not clear. Between trimers there are no contacts in the (*a*,*b*) plane and thus protein–lipid–protein interactions must play a key role in the order and stability of this plane. Contacts along the *c* axis are sparse and provide a molecular explanation for the disorder along this axis seen in 90% of the crystals.

Published contemporaneously with the X-ray bR structure, was a structure of bR determined by electron crystallography of 2D crystals [6]. The latter structure was defined by 7842 phased amplitudes that extended to 3.0 Å resolution (90% completeness). Although the electron diffraction structure has not been refined, and electron and X-ray diffraction results are not directly comparable, the electron diffraction data set does include more terms (7842) than were used in the X-ray refinement (5893); the electron-potential densities in some of the loop regions are stronger for the electron diffraction structure than for the X-ray diffraction structure. Whether these differences are due to the completeness and resolution of the data, the extent of crystallographic refinement, or to the nature of the crystal lattice, as examples, remains to be determined. As bR is a subject common to both X-ray and electron diffraction studies, it will be enlightening to thoroughly compare and contrast the results obtained using these fundamental tools.

In the electron-density map from the X-ray data a number of key groups involved in proton pumping are clearly defined: retinal and its Schiff base partner Lys216; Asp85, the residue that accepts the proton from the Schiff base during the photocycle; Asp96, the indirect proton donor to the Schiff base; and other residues on the extracellular side of the channel, such as Arg82 and Glu204 [27]. New results from the X-ray study, which contradict those of previous studies, show that Arg82 is not close enough to Asp85 to form a salt bridge and that Glu204 points away from the extracellular mouth of the proton channel. Reinforcing the conclusion from previous structural studies, the X-ray diffraction data shows that some of the residues implicated in proton translocation are too far apart to participate in direct proton transfer.

One of the major contributions of the X-ray structure is in the determination of the location of water molecules that bridge key residues and presumably participate in proton translocation [27]. A pocket of well defined water molecules located near Asp85 probably participates in proton transfer from Asp85 to Arg82 and Thr205. Making hydrogen bonds to the backbone carbonyl of Lys216 and the amide of Val217 is another ordered water molecule, the role of which may be to stabilize the somewhat distorted conformation of helix G. On the cytoplasmic side of the chromophore, located between the Schiff base and Asp96, is another water molecule that most likely mediates a proton transfer between Asp96 and the Schiff base during a late step in the photocycle.

### The mechanism of proton pumping

bR is a light-driven proton pump that couples the isomerization of all-*trans* retinal to the translocation of a proton from the cytoplasm to the extracellular space via multiple and discrete spectroscopic and conformational states [11, 13,30]. The structure that Pebay-Peyroula *et al.* have determined is representative of the ground state in which the retinal chromophore is protonated [27]. Although low resolution structural studies [31] as well as other experiments indicate that significant conformational changes occur throughout the photocycle, the structure of the ground state, nonetheless, provides information with which to refine the mechanism of proton translocation.

Pebay-Peyroula and colleagues propose that upon retinal isomerization the position of Trp86 changes, disrupting its interaction with Asp85 and thus allowing Asp85 to

reposition closer to the Schiff base and to directly accept the proton (see Figure 5). Water molecules hydrogen bonded to Asp85, Tyr57, Asp212 and Arg82 participate in the multiple-path transfer of the proton from Asp85 to Arg82 and Thr205. Located near the cytoplasmic mouth of the channel, and within 5 Å of Thr205, Glu9 may release the proton to the extracellular medium. In addition to the above outlined pathway, the proton release pathway may involve transfer of the proton from Arg82 to Glu204, possibly via an intervening water molecule, and then to Glu9, Glu74 or Glu194 before release to the bulk solution [6].

There is unequivocal evidence to show that Asp96, which has a p$K_a$ of ~11 and is protonated in the ground state, serves as the proton source for reprotonation of the Schiff base at a late stage in the photocycle (see for example [32]). How does this occur? Asp96 is located ~10 Å from the Schiff base and the X-ray data does not reveal a series of amino acids or water molecules that could transfer the proton. Thus, conformational rearrangement of protein sidechains and water molecules during the photocycle may be one means by which proton conductivity between Asp96 and the Schiff base is attained. Closer to the cytoplasm, Asp38 is proximal to Asp96 and serves as the proton donor to Asp96 [33]. Additional aspartate residues, that include Asp36, Asp102 and Asp104, surround Asp38 at the cytoplasmic entrance to the proton channel and probably serve as proton sources for Asp38 [6].

As emphasized by Kimura and coworkers, "The mechanism of proton transfer on the cytoplasmic side contrasts strongly with that on the extracellular side: aspartate versus glutamate layout; converging versus diverging pathway; and lateral versus longitudinal transfer, respectively, but both mechanisms have the possibility of multiple pathways" [6]. The degeneracy of the proton transfer pathways deduced from the structural studies is consistent with point-mutation studies which show that single mutations generally do not have a strong influence on the proton pumping activity of bR.

Permission to reproduce this figure in the electronic version of the manuscript was denied.

**Figure 5**

Proton translocation pathway and retinal-binding pocket.
(a) Schematic representation of the residues and solvent molecules that define or neighbor the proton channel. Water molecules depicted as solid blue circles are well defined in the model and have B values less than the mean B value for the protein; water molecules defined by open blue circles refine with high B values (~100 Å$^2$). The distances from water molecule 5 to the Schiff base nitrogen, from Asp38 to Asp96, and from Thr205 to Glu9 are shown with arrows. Water molecule 7 is 4.2 Å from Asp85. (b) All-*trans* retinal is built into an electron-density map calculated using ($2F_o$–$F_c$) coefficients, contoured at 1σ, and including terms to 2.5 Å resolution. The nature and composition of the retinal-binding pocket is similar to that determined from the electron crystallography structure [5]. (The figure and legend were adapted from [27] with permission.)

### Implications for membrane protein crystallization

The crystallization of bR using lipidic cubic phases is an important advance in membrane protein crystallization because it provides a means to grow type I crystals. As a consequence, it may change the strategies by which membrane proteins are crystallized in the future. In fact, until now, there has been no systematic effort focused on methods for the growth of type I crystals of membrane proteins. Landau and Rosenbusch have provided the field with several major advances: an X-ray structure of bR; a demonstration of one lipidic cubic phase, $Q^{224}$, and two types of lipids, 1-monooleoyl-*rac*-glycerol and 1-monopalmitoleoyl-*rac*-glycerol, that produce bR crystals; and a novel strategy to crystallize membrane proteins in a bilayer or bilayer-like environment. Indeed, Landau and Rosenbusch indicated that the instability of many membrane proteins outside of a bilayer motivated their pursuit of a membrane-like context for crystallization [14].

Further experimentation will determine the utility of lipidic cubic phases in the crystallization of other membrane proteins. Given the typical difficulty in forming well-ordered crystals of a membrane protein, however, lipidic cubic phases offer a strategy that may be considered orthogonal to typical approaches and thus will explore a different region of crystallization space. Future developments in the growth of type I membrane protein crystals via lipidic cubic phases may include the use of different lipids, the inclusion of various additives, the development of different types of crystallization screens, and the rational introduction of covalent or noncovalent lattice contacts.

### Acknowledgements

Eva Pebay-Peyroula's figures, and the helpful comments of M Krebs and B Ramachandran are greatly appreciated. Support for the author's studies on membrane proteins comes from the National Institutes of Health (NIH), Office of Naval Research (ONR), National Science Foundation (NSF) and the Sloan Foundation.

### References

1. Frost, R. In *The Poetry of Robert Frost*. Editor, E.C. Lathem. Henry Holt and Co. New York, 1969.
2. Oesterhelt, D. & Stoeckenius, W. (1971). Rhodopsin-like protein from the purple membrane of *Halobacterium halobium*. *Nat. New Biol.* 233, 149–152.
3. Blaurock, A.E. & Stoeckenius, W. (1971). Structure of the purple membrane. *Nat. New Biol.* 233, 152–154.
4. Henderson, R. & Unwin, P.N.T. (1975). Three-dimensional model of purple membrane obtained by electron microscopy. *Nature* 257, 28–32.
5. Grigorieff, N., Ceska, T.A., Downing, K.H., Baldwin, J.M. & Henderson, R. (1996). Electron-crystallographic refinement of the structure of bacteriorhodopsin. *J. Mol. Biol.* 259, 393–421.
6. Kimura, Y., *et al.*, & Fujiyoshi, Y. (1997). Surface of bacteriorhodopsin revealed by high-resolution electron crystallography. *Nature* 389, 206–211.
7. Wildenauer, D. & Khorana, H.G. (1977). The preparation of lipid-depleted bacteriorhodopsin. *Biochim. Biophys. Acta* 466, 315–324.
8. Huang, K.-S., Bayley, H., Liao, M.-J., London, E. & Khorana, H.G. (1981). Refolding of an integral membrane protein. Denaturation, renaturation and reconstitution of intact bacteriorhodopsin and two proteolytic fragments. *J. Biol. Chem.* 256, 3802–3809.
9. Khorana, H.G., *et al.*, & Biemann, K. (1979). Amino acid sequence of bacteriorhodopsin. *Proc. Natl. Acad. Sci. USA* 76, 5046–5050.
10. Ovchinnikov, Y.A., Abdulaev, N.G., Feigina, M.Y., Kiselev, A.V. & Lobanov, N.A. (1979). The structural basis of the functioning of bacteriorhodopsin: an overview. *FEBS Lett.* 100, 219–224.
11. Krebs, M.P. & Khorana, H.G. (1993). Mechanism of light-dependent proton translocation by bacteriorhodopsin. *J. Bacteriol.* 175, 1555–1560.
12. Oesterhelt, D., Tittor, J. & Bamberg, E. (1992). A unifying concept for ion translocation by retinal proteins. *J. Bioenerg. Biomembr.* 24, 181–191.
13. Lanyi, J.K. (1995). Bacteriorhodopsin as a model for proton pumps. *Nature* 375, 461–463.
14. Landau, E.M. & Rosenbusch, J.P. (1996). Lipidic cubic phases: a novel concept for the crystallization of membrane proteins. *Proc. Natl. Acad. Sci. USA* 93, 14532–14535.
15. Michel, H. & Oesterhelt, D. (1980). Three-dimensional crystals of membrane proteins: bacteriorhodopsin. *Proc. Natl. Acad. Sci. USA* 77, 1283–1285.
16. Schertler, G.F.X., Bartunik, H.D., Michel, H. & Oesterhelt, D. (1993). Orthorhombic crystal form of bacteriorhodopsin nucleated on benzamidine diffracting to 3.6 Å resolution. *J. Mol. Biol.* 234, 156–164.
17. Garavito, R.M. & Rosenbusch, J.P. (1980). Three-dimensional crystals of an integral membrane protein: an initial X-ray analysis. *J. Cell Biol.* 86, 327–329.
18. Rosenbusch, J.P. (1990). The critical role of detergents in the crystallization of membrane proteins. *J. Struct. Biol.* 104, 134–138.
19. Landau, E.M., Rummel, G., Cowan-Jacob, S.W. & Rosenbusch, J.P. (1997). Crystallization of a polar protein and small molecules from the aqueous compartment of lipidic cubic phases. *J. Phys. Chem.* 101, 1935–1937.
20. Lindblom, G. & Rilfors, L. (1989). Cubic phases and isotropic structures formed by membrane lipids – possible biological relevance. *Biochim. Biophys. Acta* 988, 221–256.
21. Luzzati, V. (1997). Biological significance of lipid polymorphism: the cubic phases. *Curr. Opin. Struct. Biol.* 7, 661–668.
22. Luzzati, V., Delacroix, H., Gulik, A., Gulik-Krzywicki, T., Mariani, P. & Vargas, R. (1997). *The Cubic Phases of Lipids*. (Vargas, R., ed.), pp. 3–24, Academic Press, San Diego, USA.
23. Landh, T. (1995). From entangled membranes to eclectic morphologies: cubic membranes as subcellular space organizers. *FEBS Lett.* 369, 13–17.
24. Michel, H. (1983). Crystallization of membrane proteins. *Trends Biochem. Sci.* 8, 56–59.
25. Henderson, R. & Shotton, D. (1980). Crystallization of purple membrane in three dimensions. *J. Mol. Biol.* 139, 99–109.
26. Cowan, S.W., *et al.*, & Rosenbusch, J.P. (1992). Crystal structures explain functional properties of two *E. coli* porins. *Nature* 358, 727–733.
27. Pebay-Peyroula, E., Rummel, G., Rosenbusch, J.P. & Landau, E.M. (1997). X-ray structure of bacteriorhodopsin at 2.5 Angstroms resolution from microcrystals grown in lipid cubic phases. *Science* 277, 1676–1681.
28. Sternberg, B., L'Hostis, C., Whiteway, C.A. & Watts, A. (1992). The essential role of specific *Halobacterium halobium* polar lipids in 2D-array formation of bacteriorhodopsin. *Biochim. Biophys. Acta* 1108, 21–30.
29. Krebs, M.P., Li, W. & Halambeck, T.P. (1997). Intramembrane substitutions in helix D of bacteriorhodopsin disrupt the purple membrane. *J. Mol. Biol.* 267, 172–183.
30. Khorana, H.G. (1993). Two light-transducing membrane proteins: bacteriorhodopsin and the mammalian rhodopsin. *Proc. Natl. Acad. Sci. USA* 90, 1166–1171.
31. Subramaniam, S., Faruqi, A.R., Oesterhelt, D. & Henderson, R. (1997). Electron diffraction studies of light-induced conformational changes in the Leu-93→Ala bacteriorhodopsin mutant. *Proc. Natl. Acad. Sci. USA* 94, 1767–1772.
32. Braiman, M.S., Mogi, T., Marti, T., Stern, L.J., Khorana, H.G. & Rothschild, K.J. (1988). Vibrational spectroscopy of bacteriorhodopsin mutants: light-driven proton transport involves protonation changes of aspartic acid residues 85, 96, and 212. *Biochemistry* 27, 8516–8520.
33. Riesle, J., Oesterhelt, D., Dencher, N.A. & Heberle, J. (1996). D38 is an essential part of the proton translocation pathway in bacteriorhodopsin. *Biochemistry* 35, 6635-6643.
34. Matthews, B.W. (1968). Solvent content of protein crystals. *J. Mol. Biol.* 33, 491–497.